

Three-Loop Radiative Corrections to Lamb Shift and Hyperfine Splitting

Michael I. Eides*

*Department of Physics and Astronomy,
University of Kentucky, Lexington, KY 40506, USA, and*

*Petersburg Nuclear Physics Institute,
Gatchina, St.Petersburg 188300, Russia*

Valery A. Shelyuto†

D. I. Mendeleev Institute of Metrology, St.Petersburg 190005, Russia

Abstract

We consider three-loop radiative corrections to the Lamb shift and hyperfine splitting. Corrections of order $\alpha^3(Z\alpha)^5m$ are the largest still unknown contributions to the Lamb shift in hydrogen. We calculated radiative corrections to the Lamb shift and hyperfine splitting generated by the diagrams with insertions of one radiative photon and electron polarization loops in the graphs with two external photons. We also obtained corrections generated by the gauge invariant sets of diagrams with two reducible radiative photon insertions in the electron line and polarization operator insertion in one of the radiative photons, and diagrams with two reducible radiative photon insertions in the electron line and polarization operator insertion in one the external photons. Corrections to the Lamb shift and hyperfine splitting generated by the diagrams with insertions of the three-loop one-particle reducible diagrams with radiative photons in the electron line are calculated in the Yennie gauge.

*Electronic address: eides@pa.uky.edu, eides@thd.pnpi.spb.ru

†Electronic address: shelyuto@vniim.ru

I. INTRODUCTION

The largest still unknown contributions to the Lamb shift in hydrogen are corrections of order $\alpha^3(Z\alpha)^5m$. The magnitude of these corrections can be easily estimated multiplying the corrections of order $\alpha^2(Z\alpha)^5m$ (see, e.g., [1,2]) by an extra factor α/π . The contributions of order $\alpha^3(Z\alpha)^5m$ turn out to be as large as 1 kHz for the $1S$ state in hydrogen. Below we present our recent results for three-loop radiative corrections to the Lamb shift and hyperfine splitting.

Nonrecoil corrections of order $\alpha^3(Z\alpha)^5m$ to the Lamb shift and corrections of order $\alpha^3(Z\alpha)E_F$ to hyperfine splitting are generated by three-loop radiative insertions in the skeleton diagram in Fig. 1. Respective corrections of lower orders in α generated by one- and two-loop radiative insertions are already well known (see, e.g., review [3]). The crucial observation, which greatly facilitates further calculations, is that the scattering approximation is adequate for calculation of all corrections of order $\alpha^n(Z\alpha)^5m$ and $\alpha^n(Z\alpha)E_F$ (see, e.g., a detailed proof in [4]). One may easily understand the physical reasons which lead to this conclusion. Consider the matrix elements of the skeleton diagram in Fig. 1 with the on shell external electron lines calculated between the free electron spinors, and multiplied by the square of the Schrödinger-Coulomb wave function at the origin. They are described by the infrared divergent integral

$$-\frac{16(Z\alpha)^5}{\pi n^3} \left(\frac{m_r}{m}\right)^3 m \int_0^\infty \frac{dk}{k^4} \delta_{l0}, \quad (1)$$

in the case of the Lamb shift, and by the infrared divergent integral¹

$$\frac{8Z\alpha}{\pi n^3} E_F \int_0^\infty \frac{dk}{k^2}, \quad (3)$$

in the case of hyperfine splitting. In these integrals k is the dimensionless momentum of the exchanged photons measured in the units of the electron mass.

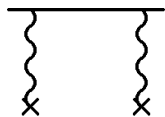


FIG. 1: Skeleton two-photon diagram

Let us consider radiative insertions in the skeleton two-photon diagram in Fig. 1. Account of these corrections effectively leads to insertion of an additional factor $L(k)$ in the divergent integrals above, and while this factor has at most a logarithmic asymptotic behavior at

¹ We define the Fermi energy E_F as

$$E_F = \frac{16}{3} Z^4 \alpha^2 \frac{m}{M} (1 + a_\mu) \left(\frac{m_r}{m}\right)^3 c h R_\infty, \quad (2)$$

where m is the electron mass, M is the muon mass, m_r is the reduced mass, α is the fine structure constant, c is the velocity of light, h is the Planck constant, R_∞ is the Rydberg constant, a_μ is the muon anomalous magnetic moment, and Z is the nucleus charge in terms of the electron charge ($Z = 1$ for hydrogen and muonium).

large momenta and does not spoil the ultraviolet convergence of the integrals, in the low-momentum region it behaves as $L(k) \sim k^2$ (again up to logarithmic factors), and improves the low-frequency behavior of the integrand. However, the integral for the Lamb shift is sometimes still divergent after inclusion of the radiative corrections because the two-photon-exchange diagram, even with radiative corrections, contains a contribution of the previous order in $Z\alpha$. This spurious contribution should be removed by subtracting the leading low-momentum term from $L(k)/k^4$. The result of such subtraction is a convergent integral, where the low integration momenta (of atomic order $mZ\alpha$) in the exchange loops are suppressed, and the effective loop integration momenta are of order m . Then it is clear that small virtuality of the external electron lines would lead to an additional suppression of the matrix element under consideration, and it is sufficient to consider the diagrams only with on-mass-shell external momenta for calculation of the contributions to the energy shifts. As an additional bonus of this approach one does not need to worry about the ultraviolet divergence of the one-loop radiative corrections. The subtraction automatically eliminates any ultraviolet divergent terms and the result is both ultraviolet and infrared finite.

II. DIAGRAMS WITH THREE ONE-LOOP ELECTRON VACUUM POLARIZATIONS

A. Lamb Shift

Each polarization loop in the diagrams in Fig. 2 corresponds to insertion of the vacuum polarization operator $(\alpha/\pi)k^2 I_{1e}$ [5] in the Lamb shift skeleton integral in eq.(1), and the contribution to the Lamb shift generated by the diagrams in Fig. 2 has the form [5]

$$\delta E_L^{(1)} = -\frac{64\alpha^3(Z\alpha)^5}{\pi^4 n^3} \left(\frac{m_r}{m}\right)^3 m \int_0^\infty dk k^2 I_{1e}^3 = -0.021\,458\,(1) \frac{\alpha^3(Z\alpha)^5}{\pi^2 n^3} \left(\frac{m_r}{m}\right)^3 m. \quad (4)$$

Numerically for the $1S$ level in hydrogen we obtain $\delta E_L^{(1)} = -0.002\,16$ kHz.

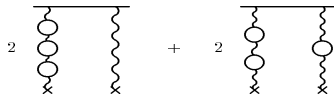


FIG. 2: Three one-loop polarizations

B. Hyperfine Splitting

We obtain the expression for the radiative correction to hyperfine splitting generated by the diagrams in Fig. 2 inserting the polarization loops in the skeleton integral in eq.(3) [5]

$$\delta E_{HFS}^{(1)} = \frac{32\alpha^3(Z\alpha)}{\pi^4 n^3} E_F \int_0^\infty dk k^4 I_{1e}^3 = 2.568\,3\,(4) \frac{\alpha^3(Z\alpha)}{\pi^2} E_F. \quad (5)$$

Numerically for the ground state in muonium the correction is $\delta E_{HFS}^{(1)} = 0.003\,29$ kHz.

III. DIAGRAMS WITH TWO-LOOP AND ONE-LOOP ELECTRON VACUUM POLARIZATIONS

A. Lamb Shift

The integral for the diagrams in Fig. 3 is obtained from the skeleton integral in eq.(1) by insertion of the one-loop vacuum polarization $(\alpha/\pi)k^2 I_{1e}$, and the two-loop vacuum polarization $(\alpha/\pi)^2 k^2 I_{2e}$ [5]

$$\delta E_L^{(2)} = -\frac{96\alpha^3(Z\alpha)^5}{\pi^4 n^3} \left(\frac{m_r}{m}\right)^3 m \int_0^\infty dk I_{1e} I_{2e} = -0.390\,152\,(7) \frac{\alpha^3(Z\alpha)^5}{\pi^2 n^3} \left(\frac{m_r}{m}\right)^3 m. \quad (6)$$

Numerically for the $1S$ level in hydrogen we obtain $\delta E_L^{(2)} = -0.039\,21$ kHz.

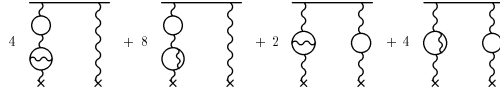


FIG. 3: One- and two-loop polarizations

B. Hyperfine Splitting

The expression for the hyperfine splitting generated by the diagrams in Fig. 3 has the form [5]

$$\delta E_{HFS}^{(2)} = \frac{48\alpha^3(Z\alpha)}{\pi^4 n^3} E_F \int_0^\infty dk k^2 I_{1e} I_{2e} = 3.559\,9\,(2) \frac{\alpha^3(Z\alpha)}{\pi^2} E_F. \quad (7)$$

Numerically for the ground state in muonium we obtain $\delta E_{HFS}^{(2)} = 0.004\,56$ kHz.

IV. DIAGRAMS WITH THREE-LOOP ELECTRON VACUUM POLARIZATION

A. Lamb Shift

For calculation of the correction generated by the diagrams in Fig. 4 we need the three-loop vacuum polarization operator $(\alpha/\pi)^3 k^2 I_{3e}$. Seven leading terms both in the low- and high-momentum asymptotic expansions of I_{3e} over the powers of the momentum were calculated analytically in [6, 7, 8, 9, 10]. We adjusted these results for the case of the momentum renormalization scheme used in QED, and constructed an interpolation which approximates the three-loop polarization operator for all Euclidean momenta.

The skeleton integral in eq.(1) remains infrared divergent even after insertion of the three-loop vacuum polarization since $I_{3e}(0) \neq 0$. This linear infrared divergence is effectively cut off at the characteristic atomic scale $mZ\alpha$ if we restore finite virtualities of the external electron lines. As mentioned in the Introduction, such infrared divergence lowers the power of the factor $Z\alpha$, and respective would be divergent contribution turns out to be of order

$\alpha^3(Z\alpha)^4$. We carry out the subtraction of the leading low-frequency asymptote of the polarization operator insertion, which corresponds to the subtraction of the leading low-frequency asymptote in the integrand for the contribution to the energy shift $\tilde{I}_{3e}(k) \equiv I_{3e}(k) - I_{3e}(0)$, and insert the subtracted expression in the formula for the Lamb shift in eq.(1). Then the contribution to the energy shift has the form [5]

$$\delta E_L^{(3)} = -\frac{32\alpha^3(Z\alpha)^5}{\pi^4 n^3} \left(\frac{m_r}{m}\right)^3 m \int_0^\infty \frac{dk}{k^2} \tilde{I}_{3e} = 1.015\,88\,(5) \frac{\alpha^3(Z\alpha)^5}{\pi^2 n^3} \left(\frac{m_r}{m}\right)^3 m. \quad (8)$$

Numerically for the $1S$ level in hydrogen we obtain $\delta E_L^{(3)} = 0.102\,10$ kHz.

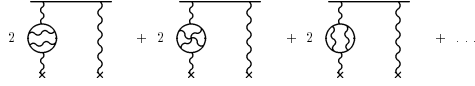


FIG. 4: Three-loop polarizations

B. Hyperfine Splitting

There is no problem of infrared divergence for the radiative correction to hyperfine splitting generated by the three-loop polarization insertions in Fig. 4 [5]

$$\delta E_{HFS}^{(3)} = \frac{16\alpha^3(Z\alpha)}{\pi^4 n^3} E_F \int_0^\infty dk I_{3e} = 1.647\,9\,(5) \frac{\alpha^3(Z\alpha)}{\pi^2} E_F. \quad (9)$$

Numerically for the ground state in muonium we obtain $\delta E_{HFS}^{(3)} = 0.002\,11$ kHz.

V. DIAGRAMS WITH ONE-LOOP ELECTRON FACTOR AND TWO ONE-LOOP ELECTRON VACUUM POLARIZATIONS

A. Lamb Shift

To calculate the correction of order $\alpha^3(Z\alpha)^5$ generated by the gauge invariant set of diagrams in Fig. 5 we need a new element, namely, the gauge invariant electron factor $L_L(k)$ in Fig. 6 which describes all possible insertions of the radiative photon in the electron line with two external photons. An explicit expression for this electron factor was obtained in different forms in [11, 12, 13, 14]. Inserting in the skeleton integral in eq.(1) the electron factor $(\alpha/\pi)k^2 L_L(k)$, one-loop polarization operator squared and the multiplicity factor 3 we obtain the radiative correction in the form

$$\delta E_L^{(4)} = -\frac{48\alpha^3(Z\alpha)^5}{\pi^4 n^3} \left(\frac{m_r}{m}\right)^3 m \int_0^\infty dk k^2 L_L(k) I_{1e}^2. \quad (10)$$

It is easy to check explicitly that this integral is both ultraviolet and infrared finite. After numerical calculations we obtain [5]

$$\delta E_L^{(4)} = 0.0773 (4) \frac{\alpha^3 (Z\alpha)^5}{\pi^2 n^3} \left(\frac{m_r}{m}\right)^3 m. \quad (11)$$

For the $1S$ level in hydrogen this contribution is $\delta E_L^{(4)} = 0.007\,77 (4)$ kHz.

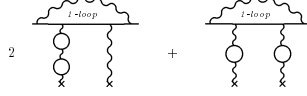


FIG. 5: One-loop electron factor and two one-loop polarizations

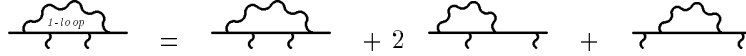


FIG. 6: One-loop electron factor

B. Hyperfine Splitting

We calculate the contribution to hyperfine splitting generated by the diagrams in Fig. 5 using an explicit expression for the electron factor L_{HFS} like in the case of the Lamb shift above. This electron factor was obtained in [15]. Inserting the electron factor $(\alpha/\pi)k^2 L_{HFS}(k)$ in the skeleton integral in eq.(3) we obtain the radiative correction in the form [5]

$$\delta E_{HFS}^{(4)} = \frac{24\alpha^3 (Z\alpha)}{\pi^4 n^3} E_F \int_0^\infty dk k^4 L_{HFS}(k) I_{1e}^2 = -3.487\,2 (2) \frac{\alpha^3 (Z\alpha)}{\pi^2} E_F. \quad (12)$$

Numerically for the ground state in muonium this contribution is $\delta E_{HFS}^{(4)} = -0.004\,47$ kHz.

VI. DIAGRAMS WITH ONE-LOOP ELECTRON FACTOR AND TWO-LOOP ELECTRON VACUUM POLARIZATION

A. Lamb Shift

An integral representation for the correction generated by the diagrams in Fig. 7 is obtained from the skeleton integral in eq.(1) in the standard way [5]

$$\delta E_L^{(5)} = -\frac{32\alpha^3 (Z\alpha)^5}{\pi^4 n^3} \left(\frac{m_r}{m}\right)^3 m \int_0^\infty dk L_L(k) I_{2e} = 2.191\,3 (4) \frac{\alpha^3 (Z\alpha)^5}{\pi^2 n^3} \left(\frac{m_r}{m}\right)^3 m. \quad (13)$$

Numerically for the $1S$ level in hydrogen this contribution is $\delta E_L^{(5)} = 0.220\,24 (4)$ kHz.

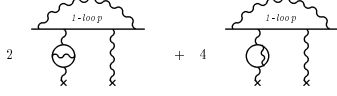


FIG. 7: One-loop electron factor and two-loop polarization

B. Hyperfine Splitting

The radiative correction to hyperfine splitting generated by the diagrams in Fig. 7 has the form [5]

$$\delta E_{HFS}^{(5)} = \frac{16\alpha^3(Z\alpha)}{\pi^4 n^3} E_F \int_0^\infty dk k^2 L_{HFS}(k) I_{2e} = -4.680\,9\,(1) \frac{\alpha^3(Z\alpha)}{\pi^2} E_F. \quad (14)$$

Numerically for the ground state in muonium we obtain $\delta E_{HFS}^{(5)} = -0.006\,00\,\text{kHz}$.

VII. DIAGRAMS WITH ONE-LOOP POLARIZATION INSERTIONS IN THE ELECTRON FACTOR AND IN THE EXTERNALAINED PHOTON

A. Lamb Shift

The contribution to the Lamb shift generated by the diagrams in Fig. 8 is similar to the contribution in eq.(13), the only difference is that now we consider a radiatively corrected electron factor in Fig. 9 and a one-loop polarization insertion in the external photon. Insertions in the skeleton integral in eq.(1) lead to the expression [5]

$$\delta E_L^{(6)} = -\frac{32\alpha^3(Z\alpha)^5}{\pi^4 n^3} \left(\frac{m_r}{m}\right)^3 m \int_0^\infty dk L_L^{(2,1)}(k) I_{1e} = 0.037\,36\,(1) \frac{\alpha^3(Z\alpha)^5}{\pi^2 n^3} \left(\frac{m_r}{m}\right)^3 m, \quad (15)$$

where the the electron factor $L^{(2,1)}$ with one-loop polarization insertion in Fig. 9 was obtained in [13]. Numerically for the $1S$ level in hydrogen this contribution is $\delta E_L^{(6)} = 0.003\,75\,\text{kHz}$.

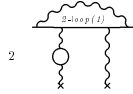


FIG. 8: One-loop polarization insertions in the electron factor and external photon

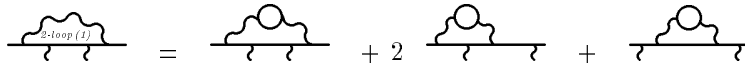


FIG. 9: One-loop polarization insertions in the electron factor

B. Hyperfine Splitting

We obtain the radiative correction to hyperfine splitting generated by the diagrams in Fig. 8 inserting the radiatively corrected electron factor $(\alpha/\pi)k^2 L_{HFS}^{(2,1)}(k)$ [16] in Fig. 9 in the skeleton integral in eq.(3) [5]

$$\delta E_{HFS}^{(6)} = \frac{16\alpha^3(Z\alpha)}{\pi^4 n^3} E_F \int_0^\infty dk k^2 L_{HFS}^{(2,1)}(k) I_{1e} = -0.533 \ 3 \ (5) \ \frac{\alpha^3(Z\alpha)}{\pi^2} E_F. \quad (16)$$

Numerically for the ground state in muonium this contribution is $\delta E_{HFS}^{(6)} = -0.000 \ 68 \text{ kHz}$.

VIII. DIAGRAMS WITH TWO ONE-LOOP POLARIZATION INSERTIONS IN THE ELECTRON FACTOR

A. Lamb Shift

The contribution to the Lamb shift generated by the diagrams in Fig. 10 is similar to the correction generated by the one-loop polarization insertion in the electron factor calculated in [13]. The explicit expression for this correction contains the electron factor with two one-loop polarization insertions $L_L^{(3,1)}(k)$ in Fig. 11 [5]

$$\delta E_L^{(7)} = -\frac{16\alpha^3(Z\alpha)^5}{\pi^4 n^3} \left(\frac{m_r}{m}\right)^3 m \int_0^\infty dk \frac{L_L^{(3,1)}(k) - L_L^{(3,1)}(0)}{k^2} = -0.012 \ 610 \ (3) \ \frac{\alpha^3(Z\alpha)^5}{\pi^2 n^3} \left(\frac{m_r}{m}\right)^3 m. \quad (17)$$

Numerically for the $1S$ level in hydrogen we obtain $\delta E_L^{(7)} = -0.001 \ 27 \text{ kHz}$.

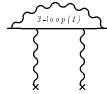


FIG. 10: One-loop polarization insertions in the electron factor

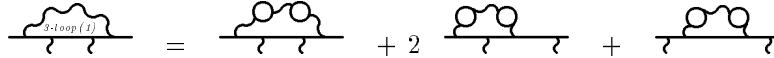


FIG. 11: Two one-loop polarization insertions in the electron factor

B. Hyperfine Splitting

The contribution to hyperfine splitting generated by the diagrams in Fig. 10 is similar to the correction generated by the one-loop polarization insertion in the electron factor which was calculated in [16]. The explicit expression for this correction has the form [5]

$$\delta E_{HFS}^{(7)} = \frac{8\alpha^3(Z\alpha)}{\pi^4 n^3} E_F \int_0^\infty dk L_{HFS}^{(3,1)}(k) = -0.309 \ 05 \ (7) \ \frac{\alpha^3(Z\alpha)}{\pi^2} E_F. \quad (18)$$

Numerically for the ground state in muonium we obtain $\delta E_{HFS}^{(7)} = -0.000\ 40$ kHz.

IX. DIAGRAMS WITH TWO-LOOP POLARIZATION INSERTION IN THE ELECTRON FACTOR

A. Lamb Shift

The contribution to the Lamb shift generated by the diagrams in Fig. 12 is similar to the correction generated by the one-loop polarization insertion in the electron factor which was calculated in [13]. The explicit expression for this correction

$$\delta E_L^{(8)} = -\frac{16\alpha^3(Z\alpha)^5}{\pi^4 n^3} \left(\frac{m_r}{m}\right)^3 m \int_0^\infty dk \frac{L_L^{(3,2)}(k) - L_L^{(3,2)}(0)}{k^2}, \quad (19)$$

differs from the respective expression in [13] only due to the difference between the electron factor with one-loop polarization insertion $L_L^{(2,1)}(k)$ in Fig. 9 and the electron factor with the two-loop polarization insertion $L_L^{(3,2)}(k)$ in Fig. 13. After numerical calculations we obtain [5]

$$\delta E_L^{(8)} = -0.245\ 71\ (7) \frac{\alpha^3(Z\alpha)^5}{\pi^2 n^3} \left(\frac{m_r}{m}\right)^3 m. \quad (20)$$

For the $1S$ level in hydrogen the correction is $\delta E_L^{(8)} = -0.024\ 70$ kHz.

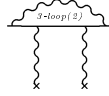


FIG. 12: Two-loop polarization insertions in the electron factor

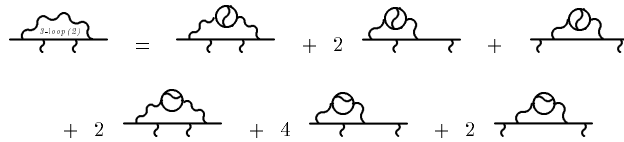


FIG. 13: Two-loop polarization insertions in the electron factor

B. Hyperfine Splitting

The contribution to hyperfine splitting generated by the diagrams in Fig. 12 is similar to the correction generated by the one-loop polarization insertion in the electron factor which was calculated in [16]. The explicit expression for this correction has the form [5]

$$\delta E_{HFS}^{(8)} = \frac{8\alpha^3(Z\alpha)}{\pi^4 n^3} E_F \int_0^\infty dk L_{HFS}^{(3,2)}(k) = -0.123\ 9\ (6) \frac{\alpha^3(Z\alpha)}{\pi^2} E_F. \quad (21)$$

Numerically for the ground state in muonium we obtain $\delta E_{HFS}^{(8)} = -0.000\ 16$ kHz.

X. DIAGRAMS WITH FACTORIZED RADIATIVE PHOTONS AND POLARIZATION OPERATOR INSERTIONS IN ONE THE RADIATIVE PHOTONS

A. Lamb shift

We use representations

$$\Lambda_\mu(k, \tau) = \frac{\alpha}{2\pi} \left\{ A_\tau \mathbf{k}^2 \gamma_\mu + B_\tau \gamma_\mu (\hat{p} - \hat{k} - m) + C_\tau p_\mu (\hat{p} - \hat{k} - m) + E_\tau \sigma_{\mu\lambda} k^\lambda \right\}, \quad (22)$$

$$\Sigma(p - k, \tau) = \frac{\alpha}{2\pi} (\hat{p} - \hat{k} - m)^2 \left[M_{\tau 1} + (\hat{p} - \hat{k}) M_{\tau 2} \right],$$

for one-loop vertex and mass operator with massive photon, and similar representations $\Lambda_\mu(k)$ and $\Sigma(p - k)$ for one-loop vertex and mass operator with massless photon to obtain an explicit expression for the contribution to the Lamb shift generated by the diagrams in Fig. 14

$$\begin{aligned} \delta E_L^{(9)} = & \frac{4\alpha^3(Z\alpha)^5}{\pi^4 n^3} \left(\frac{m_r}{m} \right)^3 m \int_0^1 dv \frac{v^2 \left(1 - \frac{v^2}{3} \right)}{1 - v^2} \int dX \int_0^\infty dk [(-A + B + C - E + M_1)(A_\tau - M_{\tau 2}) \\ & + (-A_\tau + B_\tau + C_\tau - E_\tau + M_{\tau 1})(A - M_2)] = -0.139 \ 97 \ (1) \ \frac{\alpha^3(Z\alpha)^5}{\pi^2 n^3} \left(\frac{m_r}{m} \right)^3 m. \end{aligned}$$

Numerically for the $1S$ level in hydrogen this correction is $\delta E_L^{(9)} = -0.014 \ 07$ kHz.

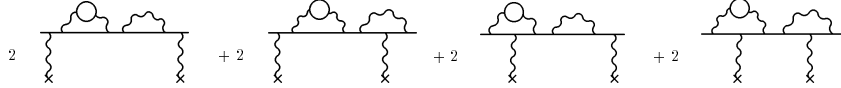


FIG. 14: One-loop polarization insertions in one of the radiative photons

B. Hyperfine Splitting

The contribution to hyperfine splitting generated by the diagrams in Fig. 14 has the form

$$\begin{aligned} \delta E_{HFS}^{(9)} = & \frac{2\alpha^3(Z\alpha)}{\pi^4 n^3} E_F \int_0^1 dv \frac{v^2 \left(1 - \frac{v^2}{3} \right)}{1 - v^2} \int dX \int_0^\infty dk [2\mathbf{k}^2 A A_\tau - 2(A E_\tau + A_\tau E) \quad (23) \\ & - 2(B B_\tau - B E_\tau - E B_\tau + E E_\tau) + C(E_\tau - B_\tau) + C_\tau(E - B) - 2\mathbf{k}^2 A M_{\tau 2} + (2B + C)(-M_{\tau 1} + M_{\tau 2}) \\ & + 2E M_{\tau 1} - 2\mathbf{k}^2 A_\tau M_2 + (2B_\tau + C_\tau)(-M_1 + M_2) + 2E_\tau M_1 - 2(M_1 - M_2)(M_{\tau 1} - M_{\tau 2}) + 2\mathbf{k}^2 M_2 M_{\tau 2}]. \\ & = 0.051 \ 44 \ (4) \ \frac{\alpha^3(Z\alpha)}{\pi^2 n^3} E_F. \end{aligned}$$

Numerically for the ground state in muonium we obtain $\delta E_{HFS}^{(9)} = 0.000 \ 07$ kHz.

XI. DIAGRAMS WITH FACTORIZED RADIATIVE PHOTONS AND POLARIZATION OPERATOR INSERTIONS IN ONE THE EXTERNAL PHOTONS

A. Lamb shift

The contribution to the Lamb shift generated by the diagrams in Fig. 15 in terms of one-loop radiative corrections has the form

$$\delta E_L^{(10)} = \frac{4\alpha^3(Z\alpha)^5}{\pi^4 n^3} \left(\frac{m_r}{m}\right)^3 m \int_0^1 dv \int_0^\infty dk \frac{k^2 v^2 \left(1 - \frac{v^2}{3}\right)}{4 + k^2(1 - v^2)} \int dX [(-A+B+C-E+M_1)(A-M_2) \\ + (-A+B+C-E+M_1)(A-M_2)] = -0.006\,25\,(1) \frac{\alpha^3(Z\alpha)^5}{\pi^2 n^3} m.$$

Numerically for the $1S$ level in hydrogen we obtain $\delta E_L^{(10)} = -0.000\,63$ kHz.

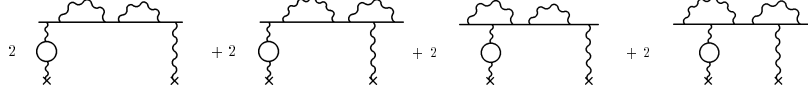


FIG. 15: One-loop polarization insertions in one of the external photons

B. Hyperfine Splitting

The contribution to hyperfine splitting generated by the diagrams in Fig. 15 has the form

$$\delta E_{HFS}^{(10)} = \frac{2\alpha^3(Z\alpha)}{\pi^4 n^3} E_F \int_0^1 dv \int_0^\infty dk \frac{k^2 v^2 \left(1 - \frac{v^2}{3}\right)}{4 + k^2(1 - v^2)} \int dX [2\mathbf{k}^2 A^2 - 4AE \\ - 2(B^2 - 2BE + E^2) + 2C(E - B) - 2\mathbf{k}^2 AM_2 + (2B + C)(-M_1 + M_2) \\ + 2EM_1 - 2\mathbf{k}^2 AM_2 + (2B + C)(-M_1 + M_2) + 2EM_1 - 2(M_1 - M_2)^2 + 2\mathbf{k}^2 M_2^2] \\ = 0.024\,8\,(5) \frac{\alpha^3(Z\alpha)}{\pi^2 n^3} E_F. \quad (24)$$

Numerically for the ground state in muonium we obtain $\delta E_{HFS}^{(10)} = 0.000\,03$ kHz.

XII. DISCUSSION OF RESULTS

We calculated three-loop radiative corrections to the Lamb shift of order $\alpha^3(Z\alpha)^5 m$ and three-loop radiative corrections to hyperfine splitting of order $\alpha^3(Z\alpha) E_F$ generated by the gauge invariant sets of diagrams in Figs. 2, 3, 4, 5, 7, 8, 10, 12, 14, and 15. Collecting all contributions above we obtain

$$\delta E_L = \sum_{i=1}^{i=10} \delta E_L^{(i)} = 2.5057 \frac{\alpha^3(Z\alpha)^5}{\pi^2 n^3} m. \quad (25)$$

Numerically for the $1S$ level in hydrogen this contribution is $\delta E_L = 0.252$ kHz.

For hyperfine splitting we obtain

$$\delta E_{HFS} = \sum_{i=1}^{i=10} \delta E_{HFS}^{(i)} = -1.282 \frac{\alpha^3(Z\alpha)}{\pi^2 n^3} E_F. \quad (26)$$

Numerically for the ground state in muonium the contribution is $\delta E_{HFS} = -0.0017$ kHz.

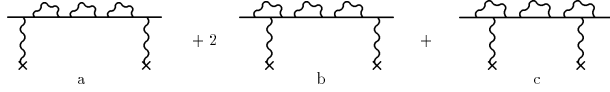


FIG. 16: Reducible three-loop diagrams

We also calculated corrections of order $\alpha^3(Z\alpha)^5 m$ to the Lamb shift and corrections of order $\alpha^3(Z\alpha)E_F$ to hyperfine splitting generated by the diagrams in Fig. 16. These factorized contributions are not gauge invariant and calculations we made in the Yennie gauge. We obtained [17]

$$\Delta E_L = -5.32193(1) \frac{\alpha^3(Z\alpha)^5}{\pi^2 n^3} \left(\frac{m_r}{m}\right)^3 m, \quad (27)$$

or $\Delta E_L = -0.535$ kHz for the $1S$ level in hydrogen.

Respective contribution to hyperfine splitting is [17]

$$\Delta E_{HFS} = 0.10423(1) \frac{\alpha^3(Z\alpha)}{\pi^2} E_F, \quad (28)$$

or $\Delta E_{HFS} = 0.00013$ kHz for the ground state in muonium.

Work on calculation of the remaining three-loop contributions to the Lamb shift and hyperfine splitting is now in progress.

Acknowledgments

This work was supported in part by the NSF grant PHY-0456462. The work of V. A. Shelyuto was also supported in part by the RFBR grants 06-02-16156 and 06-02-04018, and by the DFG grant GZ 436 RUS 113/769/0-2.

-
- [1] K. Pachucki, Phys. Rev. Lett. **72**, 3154 (1994).
 - [2] M. I. Eides and V. A. Shelyuto, Phys. Rev. A **52**, 954 (1995).
 - [3] M. I. Eides, H. Grotch, and V. A. Shelyuto, Phys. Rep. **342**, 63 (2001).
 - [4] M. I. Eides, S. G. Karshenboim, and V. A. Shelyuto, Ann. Phys. (NY) **205**, 231 (1991).
 - [5] M. I. Eides and V. A. Shelyuto, Phys. Rev. A **68**, 042106 (2003).
 - [6] P. A. Baikov and D. J. Broadhurst, preprint OUT-4102-54, hep-ph 9504398, April 1995, published in the proceedings *New Computing Technique in Physics Research IV*, ed. B. Denby and D. Perret-Gallix, World Scientific, 1995.
 - [7] P. A. Baikov, Phys. Lett. B **385**, 404 (1996).

- [8] K. G. Chetyrkin, J. H. Kühn, and M. Steinhauser, Nucl. Phys. B **482**, 213 (1996).
- [9] K. G. Chetyrkin, R. Harlander, J. H. Kühn, and M. Steinhauser, Nucl. Instr. Meth. Phys. Res. A **389**, 354 (1997).
- [10] K. G. Chetyrkin, R. Harlander, J. H. Kühn, and M. Steinhauser, Nucl. Phys. B **503**, 354 (1997).
- [11] G. Bhatt and H. Grotch, Ann. Phys. (NY) **178**, 1 (1987).
- [12] M. I. Eides and H. Grotch, Phys. Lett. B **301**, 127 (1993).
- [13] M. I. Eides and H. Grotch, Phys. Lett. B **308**, 389 (1993).
- [14] M. I. Eides, H. Grotch, and V. A. Shelyuto, Phys. Rev. A **55**, 2447 (1997).
- [15] M. I. Eides, S. G. Karshenboim, and V. A. Shelyuto, Phys. Lett. B **229**, 285 (1989); Pis'ma Zh. Eksp. Teor. Fiz. **50**, 3 (1989) [JETP Lett. **50**, 1 (1989)]; Yad. Fiz. **50**, 1636 (1989) [Sov. J. Nucl. Phys. **50**, 1015 (1989)].
- [16] M. I. Eides, S. G. Karshenboim, and V. A. Shelyuto, Phys. Lett. B **249**, 519 (1990)
- [17] M. I. Eides and V. A. Shelyuto, Phys. Rev. A **70**, 022506 (2004).